Classical and quantum interference in multiband optical Bloch oscillations

Stefano Longhi[*]

Dipartimento di Fisica and Istituto di Fotonica e Nanotecnologie del CNR, Politecnico di Milano,
Piazza L. da Vinci 32, I-20133 Milano, Italy

Classical and quantum interference of light propagating in arrays of coupled waveguides and undergoing multiband optical Bloch oscillations (BOs) with negligible Zener tunneling is theoretically investigated. In particular, it is shown that Mach-Zehnder-like interference effects spontaneously arise in multiband BOs owing to beam splitting and subsequent beam recombination occurring in one BO cycle. As a noteworthy example of quantum interference, we discuss the doubling of interference fringes in photon counting rates for a correlated photon pair undergoing two-band BOs, a phenomenon analogous to the manifestation of the de Broglie wavelength of an entangled biphoton state observed in quantum Mach-Zehnder interferometry.

I. INTRODUCTION

Since the pioneering works by Bloch, Zener, and Wannier on the coherent electron dynamics in biased crystalline solids,[1] it is well established that quantum particles in periodic potentials subjected to an external force do not delocalize but undergo a high-frequency oscillatory motion known as a Bloch oscillation (BO). Tunneling to higher-order bands, referred to as Zener tunneling (ZT) and observed for a strong external bias, is responsible for BO damping and broadening of Wannier-Stark resonances. Owing to detrimental dephasing and many-body effects, the experimental verification of BOs failed for many decades. Nowadays BOs are considered a rather universal wavy phenomenon and their observation has been reported in different physical systems for both quantum particles and classical waves. In the quantum realm, BOs have been observed for electrons in biased semiconductor superlattices[2] and for Bose-Einstein condensates in accelerating optical lattices.[3] Classical analogs of BOs, based on interference effects of classical waves in periodic media, have been proposed and experimentally observed using either optical[4–7] or acoustical[8] waves. Optical BOs in artificial materials or at the nanoscale have been also recently predicted.[9] Among various photonic structures, arrays of coupled waveguides with transverse refractive index gradients have provided an extremely rich laboratory tool to visualize the classical wave optic analogs of BOs (Refs. 4, 6, and 7) and related phenomena, such as the coherent superposition of BOs and ZT (the so-called Bloch-Zener oscillations[10]) occurring in binary structures and recently observed in circularly curved femtosecond-laser-written waveguide arrays.[11] In another physical context, application of Bloch-Zener oscillations to matter-wave interferometry has also been proposed.[12] While there has been a lot of interest in the propagation of light waves in complex photonic structures such as lattices and superlattices, quasicrystals, and even random lattices, most of the previous works focused on the propagation of classical light and used the photonic structures as "classical simulators" of electronic or matter-wave systems in periodic or random potentials. However, it is known that the coupled waveguides behave similarly to beam splitters (see, for instance, Ref. 13) and may therefore show quantum interference effects when probed with nonclassical light. The demonstration of key quantum effects of nonclassical light in silicon-based waveguide circuits has been recently reported in Ref. 14. As shown in recent works,[15,16] nonclassical light consisting of only particlelike quanta propagating in waveguide arrays with a superimposed transverse refractive index gradient can also produce optical BOs. Remarkably, in addition to the classical wave Bragg scattering the quantum nature of light introduces new quantum interference effects. In particular, two-photon Hong-Ou-Mandel quantum interference[17] has been predicted for pairs of correlated photons undergoing Bloch-Zener oscillations in binary arrays. Here ZT periodically mixes photons belonging to the two minibands of the array and thus acts like a beam splitter.[15] Recently, quantum correlations of photon pairs undergoing discrete diffraction in homogeneous arrays have been investigated as well, and their classical counterpart has been experimentally observed in the Hanbury Brown-Twiss intensity correlation measurements.[18] The investigation of quantum interference effects in complex photonic structures such as homogeneous, inhomogeneous, or even random photonic lattices has two main motivations. On one hand, they may offer the possibility of engineering photon entanglement and of transporting nonclassical light;[18,19] on the other hand, they enable to utilize optical-quantum analogies in the opposite direction, i.e., trying to observe quantum version of classical wave phenomena (such as the analog of the Talbot effect in the second-quantized setup[19]).

It is the aim of this work to provide a comprehensive analysis of classical and quantum interference of light undergoing BOs in inhomogeneous waveguide arrays in the regime of multiband excitation and negligible ZT, i.e., in a complementary regime of that previously considered in Refs. 12 and 15. In spite of the absence of interband transitions, it is shown that Mach-Zehnder-like interference effects do spontaneously occur for a multiband excitation of the array at the input plane. In this regime, the input beam breaks up into two (or more) wave packets belonging to different bands of the array which follow distinct paths in the real space and recombine after a full BO cycle. Wave and photon interference effects after a full BO cycle may be thus observed by classical and nonclassical light illumination, even in the absence of ZT. In particular, it is shown that array excitation
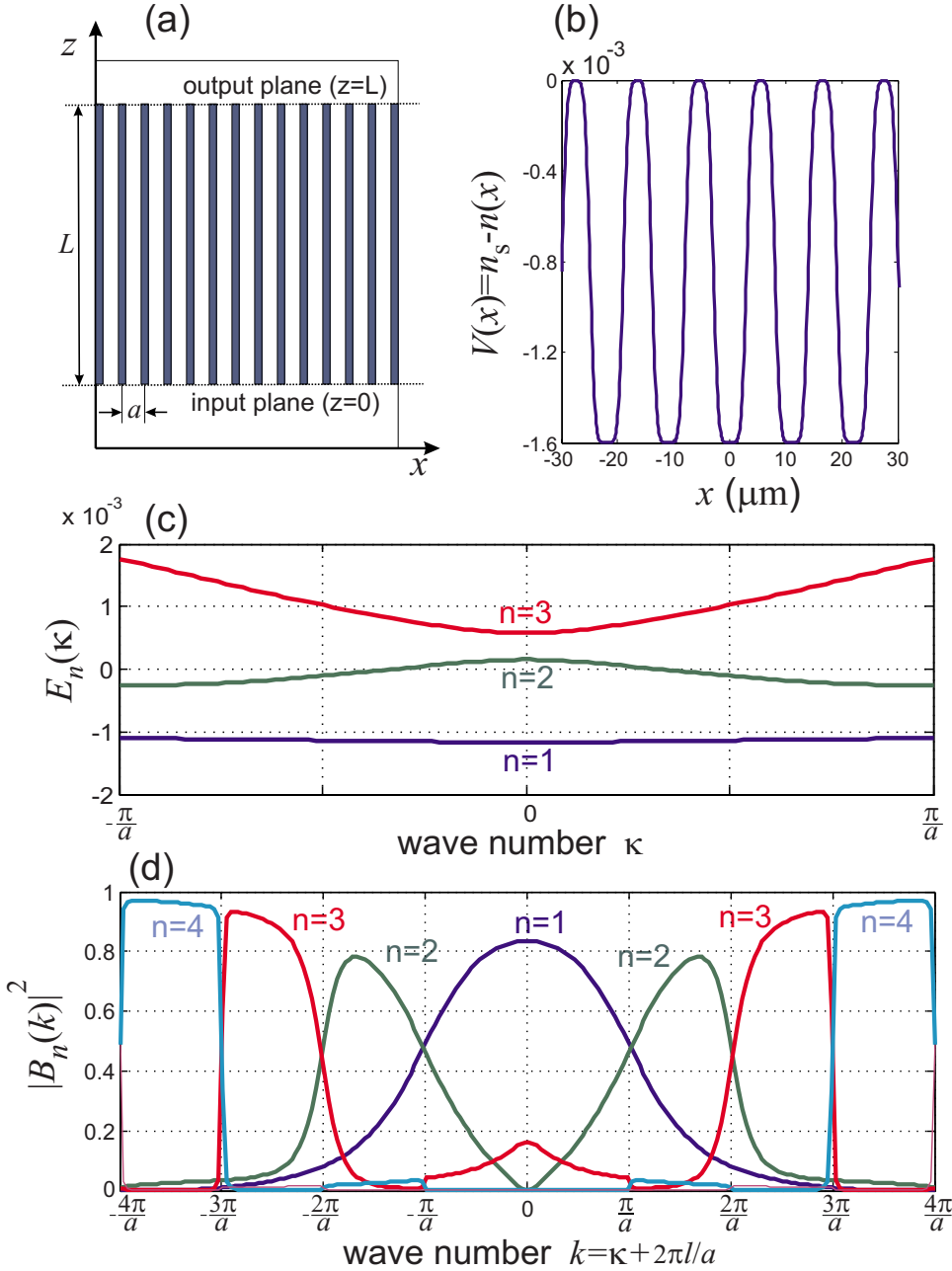
FIG. 1. (Color online) (a) Schematic of a singly-periodic one-dimensional waveguide array. (b) Behavior of the array refractive index $V(x)=n_s-n(x)$ used in numerical simulations. The transverse index ramp term is applied by, e.g., transverse thermal heating or by circularly curving the waveguide axis (not shown in the figure). (c) Band diagram. (d) Behavior of the Fourier coefficients $|B_n(k=\kappa+2\pi l/a)|^2=|\theta_{n,l}(\kappa)|^2$ of Bloch modes $\varphi_n(x,\kappa)$ for a few low-order bands.

with correlated photon pairs tilted at the Bragg angles enables to observe the quantum interference patterns in two-photon correlation measurements analogous to those occurring in quantum Mach-Zehnder interferometry as a manifestation of the de Broglie wavelength of entangled photon states.[20–23]

II. WAVE-OPTICS MODEL OF MULTIBAND BLOCH OSCILLATIONS IN A WAVEGUIDE ARRAY

The starting point of our analysis is provided by a rather standard wave optics model describing BOs of monochromatic light waves at carrier frequency $\omega=2\pi c_0/\lambda$ propagating in a weakling guiding one-dimensional waveguide array [Fig. 1(a)], with a periodic refractive index profile $n(x)$ and with a superimposed transverse refractive index gradient

Fx.[7,15,24] In the paraxial approximation, the slow evolution of a scalar field component $\phi(x,z)$ along the paraxial z direction is governed by the Schrödinger-like wave equation (see, for instance, Ref. 24),

$$i\lambdabar\phi_z=-\frac{\lambdabar^2}{2n_s}\phi_{xx}+[V(x)-Fx]\phi, \qquad (1)$$

where $\lambdabar=\lambda/(2\pi)$ is the reduced wavelength, n_s is the substrate refractive index, $V(x)=n_s-n(x)$ accounts for the periodic modulation of the refractive index with spatial periodicity a $[V(x+a)=V(x)]$, and F is the superimposed transverse index gradient. The array is assumed to be confined in the region $0<z<L$ [see Fig. 1(a)] and array excitation is accomplished at the input plane $z=0$. Since $V(x)=F=0$ for $z<0$ and $z>L$, usual paraxial diffraction occurs before and after

the light beam enters and leaves the arrayed structure. The sample length L is typically chosen to be equal to the characteristic period z_B of BOs at a reference value $F=F_0$ of index gradient, i.e., $L=z_B$ where[24]

$$z_B = \frac{\lambda}{Fa}. \tag{2}$$

In the absence of the transverse index gradient ($F=0$), the modes of the arrayed structure are the Bloch states $\varphi_n(x,\kappa)$ with corresponding dispersion curves $E_n(\kappa)$, where $n=1,2,3,\ldots$ is the band index, κ is the Bloch wave number (quasimomentum) which varies in the first Brillouin zone $-\pi/a < \kappa \le \pi/a$, and the orthogonal and normalization conditions $\langle \varphi_{n'}(x,\kappa') | \varphi_n(x,\kappa) \rangle = \delta_{n,n'} \delta(\kappa-\kappa')$ hold. $\varphi_n(x,\kappa)$ and $E_n(\kappa)$ are found as eigenfunctions and eigenvalues of the problem $\mathcal{H}_0 \varphi_n(x,\kappa) = E_n(\kappa)\varphi_n(x,\kappa)$ with periodic Hamiltonian $\mathcal{H}_0 = -[\lambda^2/(2n_s)]\partial_{xx}^2 + V(x)$. According to the Bloch theorem, one can write $\varphi_n(x,\kappa) = u_n(x,\kappa)\exp(i\kappa x)$, where the periodic part $u_n(x,\kappa)$ of the Bloch state can be expanded as a Fourier series,

$$u_n(x,\kappa) = \frac{1}{\sqrt{2\pi}} \sum_{l=-\infty}^{\infty} \theta_{n,l}(\kappa) \exp[(2i\pi l/a)x], \tag{3}$$

with coefficients $\theta_{n,l}(\kappa)$. Owing to the orthogonal and normalization conditions of Bloch states, the matrix $\mathcal{A} \equiv \theta_{n,l}$ turns out to be unitary, i.e., $\mathcal{A}^{-1} = \mathcal{A}^{\dagger}$. In place of the Fourier coefficients $\theta_{n,l}(\kappa)$, defined in the first Brillouin zone $-\pi/a < \kappa \le \pi/a$, one can introduce the set of functions

$$B_n(k = \kappa + 2\pi l/a) = \theta_{n,l}(\kappa), \tag{4}$$

which are defined over $-\infty < k < \infty$. A typical example of the refractive index profile and corresponding band diagram is shown in Figs. 1(b) and 1(c) for an excitation wavelength $\lambda = 633$ nm, lattice period $a=11$ μm, bulk refractive index $n_s = 1.43$, and maximum index change in the waveguides $\Delta n = 0.0016$. The behavior of the Fourier coefficients $|B_n(k)|^2$ of Bloch states is also depicted in Fig. 1(d).

In the presence of a transverse index gradient F, small enough to neglect interband transitions (i.e., ZT), the solution to Eq. (1) for an assigned beam distribution $\phi(x,0)$ at the $z=0$ input plane can be written as a superposition of wave packets $\phi_n(x,z)$ belonging to the different bands of the arrays which propagate independently each other and undergo BOs, namely, one can write[24]

$$\phi(x,z) = \sum_{n=1,2,3,\ldots} \phi_n(x,z). \tag{5}$$

For negligible ZT, the evolution of the wave packet ϕ_n can be calculated in a closed form by using the acceleration theorem[25] and reads[24]

$$\phi_n(x,z) = \int_{-\pi/a}^{\pi/a} d\kappa\, c_n(\kappa)\varphi_n(x,\kappa+Fz/\lambda)\exp[-i\gamma_n(\kappa,z)]. \tag{6}$$

In Eq. (6), the coefficients $c_n(\kappa)$ are determined by the field distribution illuminating the array at the input plane according to

$$c_n(\kappa) = \langle \varphi_n(x,\kappa) | \phi(x,0) \rangle = \int_{-\infty}^{\infty} dx\, \varphi_n^*(x,\kappa)\phi(x,0), \tag{7}$$

whereas the phase term $\gamma_n(\kappa,z)$ is given by

$$\gamma_n(\kappa,z) = \frac{1}{F} \int_0^{Fz/\lambda} d\kappa'\, E_n'(\kappa+\kappa'), \tag{8}$$

where

$$E_n'(\kappa) = E_n(\kappa) - F\frac{2\pi}{a} \int_0^a dx\, iu_n(x,\kappa)\frac{\partial u_n(x,\kappa)}{\partial \kappa} \tag{9}$$

is the band dispersion curve, corrected to account for a possible topological (Berry phase) contribution.[26,27] In particular, after a full BO cycle, i.e., for a propagation distance $z=z_B$, one has $\phi_n(x,z_B) = \phi_n(x,0)\exp(-i\gamma_n)$, where

$$\gamma_n = \frac{1}{F} \int_0^{2\pi/a} d\kappa\, E_n'(\kappa). \tag{10}$$

Since in the general case the phases γ_n accumulated by the various wave packets ϕ_n undergoing BOs are not the same or do not differ by multiplies of 2π, the output field distribution $\phi(x,z_B)$ does not generally reproduce the input one $\phi(x,0)$. The output field is in turn given by the interference of the various wave packets $\phi_n(x,0)$ with the appropriate phase delays γ_n given by Eq. (10). This kind of interference is discussed in details in the next section and may lead to a Mach-Zehnder-like interferometry which does not require ZT.

III. BEAM BREAK UP AND RECOMBINATION: CLASSICAL INTERFERENCE

Let us consider a broad input beam, with narrow angular spectrum and near-field distribution $G(x)$, impinging the array at the incidence angle θ, so that $\phi(x,0) = G(x)\exp(i\kappa x)$ where $\kappa = n_s\theta/\lambda = (\pi/a)(\theta/\theta_B)$ and

$$\theta_B = \frac{\lambda}{2an_s} \tag{11}$$

is the Bragg angle.[28] We denote such an input field distribution as $g^{(l)}(x,0;\kappa_0)$ and the corresponding propagated field as $g^{(l)}(x,z;\kappa_0)$, where κ_0 and the integer l are defined such that $\kappa_0 + 2\pi l/a = \kappa$ and $-\pi/a \le \kappa_0 < \pi/a$. The normalization condition $\int dx |g^{(l)}(x,z;\kappa_0)|^2 = 1$ is assumed. In this case, following the analysis of Ref. 24, one can show that inside the arrayed structure one has

$$|\phi_n(x,z)|^2 = \left| \theta_{n,l}(\kappa_0)\varphi_n\left(x,\kappa_0+\frac{Fz}{\lambda}\right)G[x-x_n(z)] \right|^2, \tag{12}$$

where we have set

$$x_n(z) = \frac{1}{F}[E_n'(\kappa_0+Fz/\lambda) - E'(\kappa_0)]. \tag{13}$$

Equations (5) and (12) indicate that the injected beam $\phi(x,0)$ breaks into a superposition of wave packets ϕ_n belonging to
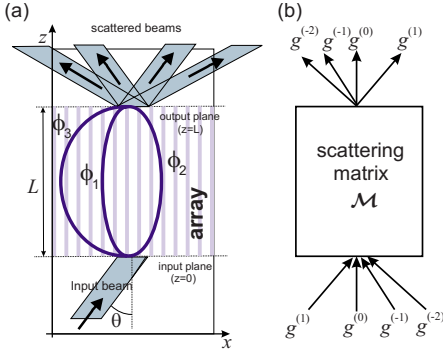
FIG. 2. (Color online) (a) Schematic of BO motion in the multiband regime. A broad beam illuminates the array at the incidence angle θ and excites several wave packets ϕ_1, ϕ_2, and ϕ_3 belonging to the different bands of the array. The wave packets undergo BOs along distinct paths which reproduce in real space the spectral shapes of the band dispersion curves. After one BO cycle, owing to different phase delays γ_n accumulated by the wave packets, several beams, diffracted at the angles $\theta, \theta \pm 2\theta_B, \theta \pm 4\theta_B, \ldots$, are produced. (b) Schematic of a linear-optic multiport system described by a scattering matrix $\mathcal{M}$.

the different bands of the array, with weighting factors $|\theta_{n,l}(\kappa_0)|^2$, which undergo BOs along different paths $x_n(z)$ [see, for instance, Figs. 3(a) and 4(a)–4(d) to be discussed below]. According to Eq. (13), the path $x_n(z)$ followed by the wave packet ϕ_n reproduces the shape of the band dispersion curve $E_n(\kappa)$, eventually corrected to include the Berry phase contribution. After a full BO cycle, i.e., at $z = z_B$, the different wave packets ϕ_n interference and the following scattering relations hold (see the Appendix):

$$g^{(l)}(x, z_B; \kappa_0) = \sum_{\rho = -\infty}^{\infty} \mathcal{M}_{l,\rho} g^{(\rho)}(x, 0; \kappa_0), \quad (14)$$

where the scattering matrix $\mathcal{M}$ is given by

$$\mathcal{M} = \mathcal{A}^\dagger \mathcal{B} \mathcal{A}, \quad \mathcal{A}_{n,l} = \theta_{n,l}(\kappa_0), \quad \mathcal{B}_{\rho,n} = \exp(-i\gamma_n)\delta_{\rho,n}, \quad (15)$$

and γ_n are given by Eq. (10). Note that if the differences of phase delays $\gamma_n - \gamma_\rho$ were multiplies of 2π, a full reconstruction of the input beam, apart from an unimportant phase term, would be achieved since $\mathcal{A}^\dagger \mathcal{A} = \mathcal{I}$. In this case the beam leaving the array at $z = z_B$ would not split and would diffract at the same tilting angle θ as that of the incoming beam. However, the phase delays γ_n do not generally satisfy the previous condition, and thus the beam leaving the array at $z = z_B$ breaks up into several beams which diffract at the different angles $\theta + 2\rho\theta_B$ ($\rho = 0, \pm 1, \pm 2, \ldots$) according to Eq. (14). After some propagation distance, such beams are not overlapped and can be thus spatially resolved. This general behavior is schematically illustrated in Fig. 2(a). More generally, we can say that if the array is simultaneously excited by a set of identical broad beams tilted at different angles $\theta + 2l\theta_B$ ($l = 0, \pm 1, \pm 2, \ldots$), the array behaves like a liner multiport optical system for the amplitudes of modes $g^{(l)}$ [see Fig. 2(b)] with a scattering matrix $\mathcal{M}$ given by Eqs. (15). Here we have focused our analysis to the case where the
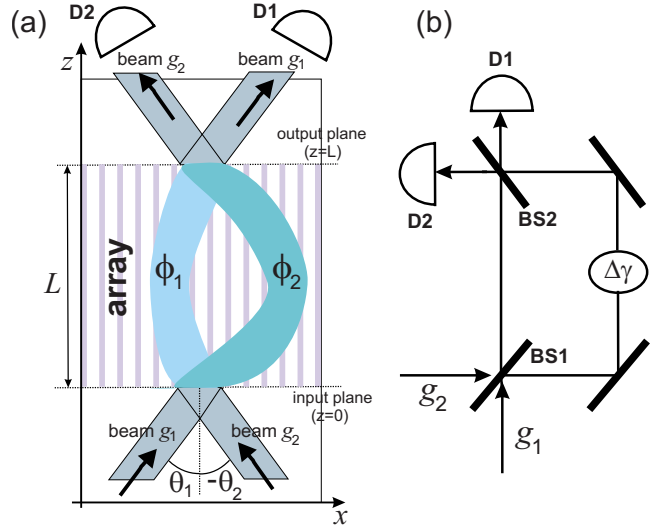

FIG. 3. (Color online) (a) Schematic of two-band BOs in a waveguide array excited by two input broad beams tilted at the angles $\theta_1 \sim \theta_B$ and $\theta_2 = \theta_1 - 2\theta_B \sim -\theta_B$. The paths followed by the wave packets ϕ_1 and ϕ_2 undergoing BOs map in real space the spectral shapes of the band dispersion curves $E_1(\kappa)$ and $E_2(\kappa)$, respectively. (b) Equivalent two-port Mach-Zehnder interferometer.

length L of the array equals the BO cycle z_B. Similar results are obtained by assuming, more generally, that the array length L comprises an integer number N of BO cycles, i.e., for $L = N z_B$. In this case, the scattering matrix can be again factorized as $\mathcal{M} = \mathcal{A}^\dagger \mathcal{B} \mathcal{A}$, where now $\mathcal{B}_{\rho,n} = \exp(-iN\gamma_n)\delta_{\rho,n}$.

As an important example, let us consider the case where only the two lowest bands of the array are involved in the dynamics, and the scattering relations (15) may be limited to two modes solely. An inspection of the curves $E_n(\kappa)$ and $|B_n(k)|^2$ shown in Figs. 1(c) and 1(d) indicates that this condition is realized, to a good approximation, when the array is excited by two broad beams tilted the former at an angle θ_1 equal to or slightly smaller than the Bragg angle θ_B, the latter at the angle $\theta_2 = \theta_1 - 2\theta_B \sim -\theta_B$ [see Fig. 3(a)]. If we use the simplified notations $g_1(x,z) \equiv g^{(0)}(x,z;\kappa_0)$ and $g_2(x,z) \equiv g^{(-1)}(x,z;\kappa_0)$ for the two modes scattered by the array in one BO cycle, where $\kappa_0 \sim \pi/a$, the input-output relations [Eq. (14)] reduce to

$$g_1(x, z_B) = S_{11} g_1(x, 0) + S_{12} g_2(x, 0), \quad (16)$$

$$g_2(x, z_B) = S_{21} g_1(x, 0) + S_{22} g_2(x, 0), \quad (17)$$

where we have set $S_{11} = \mathcal{M}_{0,0}$, $S_{12} = \mathcal{M}_{0,-1}$, $S_{21} = \mathcal{M}_{-1,0}$, and $S_{22} = \mathcal{M}_{-1,-1}$. According to Eqs. (15), the 2×2 scattering matrix S entering in Eqs. (16) and (17) is given by

$$S = \begin{pmatrix} \rho_{11}^* & \rho_{21}^* \\ \rho_{12}^* & \rho_{22}^* \end{pmatrix} \times \begin{pmatrix} \exp(-i\gamma_1) & 0 \\ 0 & \exp(-i\gamma_2) \end{pmatrix} \times \begin{pmatrix} \rho_{11} & \rho_{12} \\ \rho_{21} & \rho_{22} \end{pmatrix}, \quad (18)$$

where

$$\begin{pmatrix} \rho_{11} & \rho_{12} \\ \rho_{21} & \rho_{22} \end{pmatrix} = \begin{pmatrix} \theta_{1,0}(\kappa_0) & \theta_{1,-1}(\kappa_0) \\ \theta_{2,0}(\kappa_0) & \theta_{2,-1}(\kappa_0) \end{pmatrix}. \quad (19)$$

Since the matrix ρ_{ik} is unitary, one has $|\rho_{11}|=|\rho_{22}|$, $|\rho_{12}| = |\rho_{21}|$, $|\rho_{11}|^2 + |\rho_{12}|^2 = 1$, and $\rho_{11}\rho_{12}^* + \rho_{21}\rho_{22}^* = 0$. Without loss of generality, we may assume $\rho_{11} = \rho_{22}$ to be real valued and positive by a suitable choice of the absolute phases of $u_1(x,\kappa_0)$ and $u_2(x,\kappa_0)$. After setting $\rho_{11} = \rho_{22} = \sqrt{T}$ and $R = 1 - T$, where $T = |\theta_{1,0}(\kappa_0)|^2 = |\theta_{2,-1}(\kappa_0)|^2$, we can then write

$$\begin{pmatrix} \rho_{11} & \rho_{12} \\ \rho_{21} & \rho_{22} \end{pmatrix} = \begin{pmatrix} \sqrt{T} & \sqrt{R}\exp(i\alpha) \\ -\sqrt{R}\exp(-i\alpha) & \sqrt{T} \end{pmatrix}, \quad (20)$$

where α is the phase of ρ_{12}. Note that Eq. (20) is analogous to the scattering matrix of a lossless beam splitter with trans-mittance $T = 1 - R$ (see, for instance, Ref. 29). Physically, such a transformation corresponds to the mixing of the incoming beams g_1 and g_2 into the two wave packets ϕ_1 and ϕ_2 belonging to the two lowest-order bands of the array [see Fig. 3(a)]. At exact Bragg incidence, i.e., for $\theta_1 = -\theta_2 = \theta_B$, one has $T = 1/2$, i.e., the equivalent beam splitter is balanced. Note also that the full transformation[18] is analogous to that of a two-port Mach-Zehnder interferometer in which two waves g_1 and g_2 are mixed by a fist beam splitter BS1, undergo different phase delays γ_1 and γ_2 in the two arms of the interferometer, and are then recombined by a second beam splitter BS2 [see Fig. 3(b)]. The transfer matrix S of the equivalent Mach-Zehnder interferometer reads explicitly

$$\begin{pmatrix} S_{11} & S_{12} \\ S_{21} & S_{22} \end{pmatrix} = \begin{pmatrix} T\exp(-i\gamma_1) + R\exp(-i\gamma_2) & \sqrt{RT}\exp(i\alpha)[\exp(-i\gamma_1) - \exp(-i\gamma_2)] \\ \sqrt{RT}\exp(-i\alpha)[\exp(-i\gamma_1) - \exp(-i\gamma_2)] & T\exp(-i\gamma_2) + R\exp(-i\gamma_1) \end{pmatrix}. \quad (21)$$

Classical Mach-Zehnder interferometry, which does not require ZT, is thus expected to be observable in multiband BOs. As an example, for single beam excitation at the tilt angle θ_1, i.e., for $\phi(x,0) = g_1(x,0)$, the fractional light powers $P_1(\Delta\gamma)$ and $P_2(\Delta\gamma)$ of the two beams $g_1(x,z_B)$ and $g_2(x,z_B)$ leaving the array and measured by two photodetectors D1 and D2 [see Fig. 3(a)], are readily calculated from Eqs. (16), (17), and (21) as

$$P_1(\Delta\gamma) = |S_{11}|^2 = T^2 + R^2 + 2RT\cos(\Delta\gamma) \quad (22)$$

$$P_2(\Delta\gamma) = |S_{21}|^2 = 2RT[1 - \cos(\Delta\gamma)]. \quad (23)$$

According to Eq. (10), the phase difference $\Delta\gamma$ is given by

$$\Delta\gamma = \frac{2\pi}{Fa}\left(\frac{a}{2\pi}\int_0^{2\pi/a} d\kappa[E_2'(\kappa) - E_1'(\kappa)]\right) \equiv \frac{2\pi\Delta E}{Fa}, \quad (24)$$

where ΔE is the distance between the first and second bands of the array, measured from their dc values.[27] Typically the value ΔE is of the order of the refractive index change Δn in the core region of waveguides from the dielectric substrate [see Fig. 1(c)]. In practice, to vary $\Delta\gamma$ one can slightly change the index gradient F around the reference value $F_0 = \lambda/(aL)$.[30] In this way, the deviation of $z_B = \lambda/(Fa)$ from $L = \lambda/(F_0a)$ is negligible, i.e., the BO cycle is almost completed at the output of the arrayed region, whereas the change in $\Delta\gamma$ can be of the order of 2π or larger as Fa is typically much larger than ΔE. Figures 4(a)–4(d) show typical examples of two-band BOs observed in numerical simulations of Eq. (1) for the one-dimensional array of Fig. 1. The length of the arrayed region is $L = 23$ mm, and the condition $z_B = L$ is attained for an applied refractive index gradient $F_0 = 2.502$ m^{-1}. For such a relatively low value of refractive index gradient, ZT from band 1 to band 2, and from band 2 to band 3, turns out to be negligible. The array is excited by a broad Gaussian beam tilted at the Bragg angle $\theta_2 = -\theta_B$, and the evolution of the beam intensity $|\phi(x,z)|^2$ along the sample is plotted for a few values of the refractive index gradient F close to F_0. Beam splitting and beam recombination after a full BO cycle are clearly visible, as well as the change in the power levels in the two scattered output beams as the applied index gradient F is slightly varied (by a few percents) at around F_0. The behavior of the fractional powers P_1 and P_2 carried by the two output beams versus the ratio of F_0/F is depicted in Fig. 4(e), clearly showing an oscillatory behavior with a visibility of about ~90%.

IV. QUANTUM INTERFERENCE IN MULTIBAND BLOCH OSCILLATIONS WITH NONCLASSICAL LIGHT

In the previous sections, multiband optical BOs and interference effects have been investigated in the framework of classical electromagnetic theory. Here we extend the previous analysis to nonclassical states of light undergoing multiband BOs and discuss relevant quantum interference effects similar to those observed in the Mach-Zehnder-based quantum interferometry.[20–23] A second-quantization approach to study optical BOs in waveguide arrays, based on a procedure similar to that adopted in the quantum theory of solitons,[31] has been developed in Ref. 15. In this approach, the scalar wave equation for the classical field $\phi(x,z)$ [Eq. (1)] is written in Hamiltonian form assuming the paraxial spatial coordinate z as an independent variable, and a quantization procedure is then applied by introducing creation $\phi^\dagger(x)$ and annihilation $\phi(x)$ bosonic field operators (for details see Refs. 15 and 32). In the Schrödinger picture, the quantum field is described by a quantum state $|\mathcal{Q}(z)\rangle$ which can be expanded in Fock space as
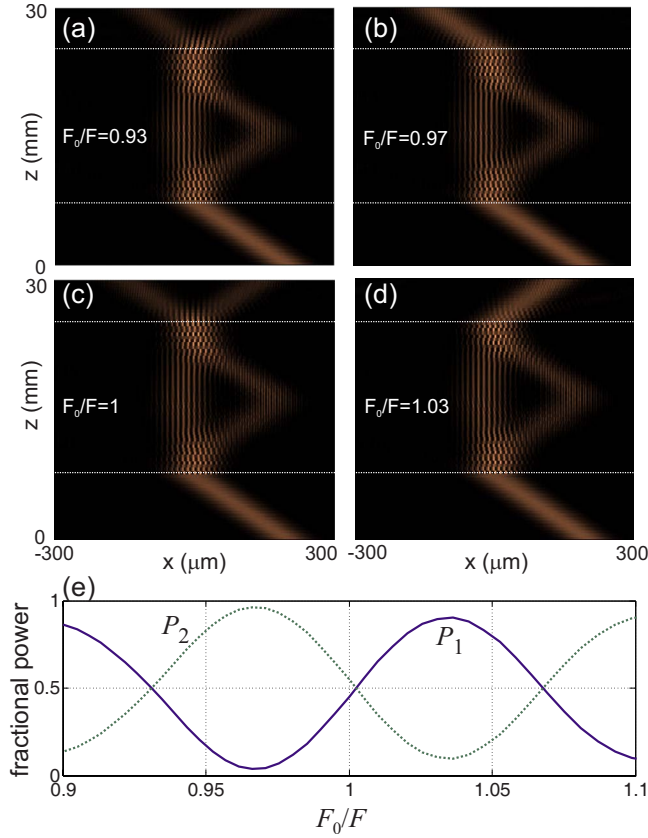
FIG. 4. (Color online) Classical Mach-Zehnder interferometry based on two-band BOs. (a)–(d) show the evolution of light intensity distribution along the optical structure, excited at the input plane by a broad Gaussian beam tilted at $\theta_2 = -\theta_B$, for a few values of F_0/F. The arrayed structure has a length $L=23$ mm and it is comprised between the two dotted horizontal lines. The index gradient F_0, at which the array length L is exactly equal to one BO cycle z_B, is given by $F_0 = 2.502$ m^{-1}. In (e) the numerically computed fractional powers P_1 and P_2 carried by the two output beams (right- and left-diffracted beams, respectively) are plotted as functions of the ratio F_0/F.

$$|\mathcal{Q}(z)\rangle = \sum_{n=1}^{\infty} a_n |f^{(n)}\rangle, \qquad (25)$$

where the n-photon number state $|f^{(n)}\rangle$ is defined by

$$|f^{(n)}\rangle = \int dx_1 dx_2 \ldots dx_n \frac{f^{(n)}(x_1, x_2, \ldots, x_n, z)}{\sqrt{n!}}$$
$$\times \hat{\phi}^\dagger(x_1)\hat{\phi}^\dagger(x_2)\ldots\hat{\phi}^\dagger(x_n)|0\rangle. \qquad (26)$$

The normalization conditions $\Sigma_n |a_n|^2 = 1$ and $\int dx_1 dx_2 \ldots dx_n |f^{(n)}(x_1, x_2, \ldots, x_n, z)|^2 = 1$ are assumed. The Fock state $|f^{(n)}\rangle$ defined by Eq. (26) is obtained from the vacuum state $|0\rangle$ by creating n photons with a spatial weighting function $f^{(n)}(x_1, x_2, \ldots, x_n, z)$. The evolution equation for $f^{(n)}$, obtained from the Schrödinger equation and using the commutation relations of field operators, reads[15]

$$i\hbar \frac{\partial f^{(n)}}{\partial z} = \sum_{l=1}^{n}\left[-\frac{\hbar^2}{2n_s}\frac{\partial^2}{\partial x_l^2} + V(x_l) - Fx_l\right]f^{(n)}. \qquad (27)$$

Owing to the bosonic nature of photons, solely symmetric functions $f^{(n)}$ should be considered. The simplest n-photon number state, denoted by $|g\rangle_n$, is obtained by assuming $f^{(n)} = g(x_1, z)g(x_2, z)\ldots g(x_n, z)$, where the function $g(x, z)$ satisfies the classical wave Eq. (1) with the normalization $\int dx |g(x, z)|^2 = 1$. Note that in this case one has

$$|g\rangle_n = \frac{1}{\sqrt{n!}}\left[\int dx\, g(x, z)\hat{\phi}^\dagger(x)\right]^n |0\rangle, \qquad (28)$$

so that this quantum state describes the excitation of the array with a beam with a spatial profile $g(x, 0)$ at the entrance plane $z=0$ and carrying n photons. More generally, for a given set of orthogonal and normalized functions $g_1(x, z), g_2(x, z), \ldots$ that satisfy Eq. (1), one can construct the n-photon number state $|g_1, g_2, \ldots\rangle_{n_1, n_2, \ldots}$ defined by

$$|g_1, g_2, \ldots\rangle_{n_1, n_2, \ldots}$$
$$= \frac{1}{\sqrt{n_1!}}\left[\int dx\, g_1(x, z)\hat{\phi}^\dagger(x)\right]^{n_1}$$
$$\times \frac{1}{\sqrt{n_2!}}\left[\int dx\, g_2(x, z)\hat{\phi}^\dagger(x)\right]^{n_2} \cdots |0\rangle, \qquad (29)$$

with $n_1 + n_2 + \cdots = n$. Such a quantum state describes the excitation of the array with a set of independent beams each carrying $n_1, n_2, \ldots$ photons ($n = n_1 + n_2 + \cdots$). The classical picture of multiband BOs, described in the previous sections, is retrieved from the quantum model when the input beam is in a coherent state (classical light), i.e., when a superposition of Fock states with a Poisson distribution is considered.[15] Here we focus to the case where the input beam describes a nonclassical field. In particular, let use suppose that the array is excited by a set of tilted beams $g^{(l)}(x, 0; \kappa_0)$ ($l = 0, \pm 1, \pm 2, \ldots$), which have been introduced in Sec. III, and assume that $g^{(l)}$ is in a photon number state (a Fock state) carrying n_l photons. After introduction of the creation operators $\hat{a}_l^\dagger$,

$$\hat{a}_l^\dagger = \int dx\, g^{(l)}(x, 0; \kappa_0)\hat{\phi}^\dagger(x), \qquad (30)$$

the quantum state of the system at the input plane of the array may be written as

$$|\mathcal{Q}(z=0)\rangle = \frac{1}{\sqrt{\ldots n_0!\, n_1!\, n_2!\, \ldots}} \cdots \hat{a}_0^{n_0}\hat{a}_1^{n_1}\hat{a}_2^{n_2}\cdots |0\rangle$$
$$\equiv |\ldots, n_0, n_1, n_2, \ldots\rangle. \qquad (31)$$

Note that as $g^{(l)}(x, 0; \kappa_0)$ are orthogonal functions, the operators $\hat{a}_l^\dagger$ and $\hat{a}_l$ satisfy the commutation relations

$$[\hat{a}_l, \hat{a}_\rho^\dagger] = \delta_{l,\rho}, \quad [\hat{a}_l, \hat{a}_\rho] = [\hat{a}_l^\dagger, \hat{a}_\rho^{ag}] = 0. \qquad (32)$$

The quantum state of the system at the output plane, i.e., after one BO cycle, can be derived from Eqs. (14) and (29), and reads explicitly

$$|\mathcal{Q}(z=z_B)\rangle = \frac{1}{\sqrt{\ldots n_0! \, n_1! \, n_2! \, \ldots}} \cdots \left(\sum_\rho \mathcal{M}_{0,\rho}\hat{a}_\rho\right)^{n_0}$$

$$\times \left(\sum_\rho \mathcal{M}_{1,\rho}\hat{a}_\rho\right)^{n_1}\left(\sum_\rho \mathcal{M}_{2,\rho}\hat{a}_\rho\right)^{n_2} \cdots |0\rangle. \qquad (33)$$

Note that since the multiband BOs problem over one BO cycle admits of a formulation in terms of a scattering matrix [Eq. (14)], the quantum state at the output plane, as given by Eq. (33), is consistent with the result that one would obtain using the input-output operator formalism commonly adopted for linear quantum-optical networks (see, for instance, Ref. 33). Equation (33) is at the basis of quantum interference and quantum entanglement observable in multiband BOs when the array is excited by photon number states. As an example, we discuss in detail the doubling of interference fringes in photon counting rates for correlated photon pairs undergoing two-band BOs, a phenomenon analogous to the doubling of interference fringes in photon correlation measurements observed in a Mach-Zehnder interferometer and attributed to the so-called de Broglie wavelength of the entangled biphoton state (see, for instance, Ref. 22). To this aim, let us consider the two-band BO problem of Fig. 3(a) discussed in Sec. III. Instead of using classical light (i.e., coherent states for the two beams g_1 and g_2), let us illuminate the array by correlated photon pairs generated by frequency-degenerate spontaneous parametric downconversion and incident onto the array at the Bragg angles $\theta_1 = \theta_B$ and $\theta_2 = -\theta_B$. The quantum state of light at the entrance plane of the array can be thus written as

$$|\mathcal{Q}(z=0)\rangle = |1\rangle_1|1\rangle_2, \qquad (34)$$

where $|n_1\rangle_1|n_2\rangle_2$ denotes a $n = n_1 + n_2$ photon number state with n_1 photons in the mode g_1 and n_2 photons in the mode g_2. Using Eqs. (16), (17), and (34), from Eqs. (31) and (33) it readily follows that the state of quantum field after one BO cycle is given by

$$|\mathcal{Q}(z=z_B)\rangle = \sqrt{2}S_{11}S_{21}|2\rangle_1|0\rangle_2 + (S_{11}S_{22} + S_{12}S_{21})|1\rangle_1|1\rangle_2$$

$$+ \sqrt{2}S_{12}S_{22}|0\rangle_1|2\rangle_2. \qquad (35)$$

The joint probabilities R_{11} and R_{22} to find both photons in the same beam, either g_1 or g_2, after one BO cycle are then given by

$$R_{11} = 2|S_{11}|^2|S_{21}|^2, \quad R_{22} = 2|S_{12}|^2|S_{22}|^2. \qquad (36)$$

Such relations give the two-photon counting rates that one would measure in an experiment.[22] Using Eq. (21) and assuming $T = R = 1/2$ (valid for incidence angles exactly tuned at the Bragg angles $\pm\theta_B$), one finally obtains

$$R_{11} = R_{22} = \frac{1}{4}[1 - \cos(2\Delta\gamma)]. \qquad (37)$$

Note that the counting rates $R_{11} = R_{22}$ oscillate like $\sim\cos(2\Delta\gamma)$, i.e., at *twice* the phase difference $\Delta\gamma$, as opposed to the classical first-order interference fringes,[34] which oscillate like $\sim\cos(\Delta\gamma)$ [see Eqs. (22) and (23)]. The doubling of the counting rate oscillation frequency versus the phase delay $\Delta\gamma$ is analogous to that observed in an ordinary

Mach-Zehnder interferometer probed by correlated photon pairs and generally explained as a manifestation of the de Broglie wavelength of the biphoton entangled state formed after the first beam splitter BS1 and probed at the second beam splitter BS2 of the interferometer.[22]

V. CONCLUSIONS

In this work interference phenomena for classical and nonclassical light propagating in arrays of coupled waveguides and undergoing multiband optical Bloch oscillations with negligible Zener tunneling have been theoretically investigated. A wave scattering analysis of multiband BOs shows that Mach-Zehnder-like interference effects spontaneously arise owing to beam splitting and subsequent beam recombination occurring at each BO cycle. A noteworthy example of quantum interference is provided by the doubling of the interference fringes in photon counting rates for a correlated photon pair undergoing two-band BOs. This phenomenon is analogous to the one observed in a Mach-Zehnder interferometer excited by pairs of correlated photons and is a manifestation of the so-called de Broglie wavelength of the two-photon entangled state produced after the first beam splitter of the interferometer and probed by the second one.[22] It is envisaged that the present results may stimulate further the theoretical and experimental investigations of the classical and quantum interference phenomena of light propagating in complex periodic, quasiperiodic, or disordered photonic lattices.

APPENDIX: DERIVATION OF THE SCATTERING MATRIX

In this appendix we derive the scattering relations given in the text [Eqs. (14) and (15)] for the amplitudes $g^{(l)}$ of tilted beams at the input and output planes of the array, i.e., after one BO cycle. To this aim, let us first prove Eqs. (14) and (15) when the incident beams are tilted plane waves, i.e., let us first assume

$$g^{(l)}(x,0;\kappa_0) = \frac{1}{\sqrt{2\pi}}\exp\left(i\kappa_0 x + i\frac{2\pi}{a}lx\right), \qquad (A1)$$

($l = 0, \pm 1, \pm 2, \ldots$). Owing to the completeness of Bloch states $\varphi_n(x,\kappa)$, one can write

$$g^{(l)}(x,0;\kappa_0) = \sum_{n=1,2,3,\ldots}\int_{-\pi/a}^{\pi/a} d\kappa \langle\varphi_n|g^{(l)}\rangle\varphi_n(x,\kappa). \quad (A2)$$

Since $\varphi_n(x,\kappa) = u_n(x,\kappa)\exp(i\kappa x)$ and taking into account the Fourier decomposition of $u_n(x,\kappa)$ [Eq. (3)], one readily finds $\langle\varphi_n(x,\kappa)|g^{(l)}(x,0;\kappa)\rangle = \theta^*_{n,l}(\kappa_0)\delta(\kappa - \kappa_0)$, so that Eq. (A2) yields

$$g^{(l)}(x,0;\kappa_0) = \sum_{n=1,2,3,\ldots}\mathcal{A}^\dagger_{l,n}\varphi_n(x,\kappa_0) \qquad (A3)$$

where we have introduced the matrix $\mathcal{A}_{n,l} \equiv \theta_{n,l}(\kappa_0)$ and $\mathcal{A}^\dagger$ is the adjoint of $\mathcal{A}$, i.e., $\mathcal{A}^\dagger_{l,n} = \mathcal{A}^*_{n,l}$. After one BO cycle, the Bloch state $\varphi_n(x,\kappa_0)$ accumulates a phase shift $\exp(-i\gamma_n)$, where γ_n is given by Eq. (10). After the introduction of the

diagonal matrix $\mathcal{B}_{\rho,n}=\exp(-i\gamma_n)\delta_{n,\rho}$, we can thus write

$$g^{(l)}(x,z_B;\kappa_0) = \sum_{n=1,2,3,\dots} \mathcal{A}^{\dagger}_{l,n}\exp(-i\gamma_n)\varphi_n(x,\kappa_0)$$

$$= \sum_{n=1,2,3,\dots}(\mathcal{A}^{\dagger}\mathcal{B})_{l,n}\varphi_n(x,\kappa_0). \quad (A4)$$

Since the matrix $\mathcal{A}$ is unitary, $\mathcal{A}^{-1}=\mathcal{A}^{\dagger}$ and Eq. (A3) can be inverted yielding

$$\varphi_n(x,\kappa_0) = \sum_{l=0,\pm1,\pm2,\dots}\mathcal{A}_{n,l}g^{(l)}(x,0;\kappa_0). \quad (A5)$$

Substitution of Eq. (A5) into Eq. (A4) finally yields

$$g^{(l)}(x,z_B;\kappa_0) = \sum_{\rho=0,\pm1,\pm2,\dots}(\mathcal{A}^{\dagger}\mathcal{B}\mathcal{A})_{l,\rho}g^{(\rho)}(x,0;\kappa_0),$$

$$(A6)$$

which are precisely the scattering relations between input and output waves given in the text [Eq. (14)], with a scattering matrix $\mathcal{M}=\mathcal{M}(\kappa_0)$ given by $\mathcal{M}=\mathcal{A}^{\dagger}\mathcal{B}\mathcal{A}$. Such relations can be extended to the case where the input waves $g^{(l)}(x,0;\kappa_0)$ are not strictly plane waves, rather tilted broad beams with a narrow angular spectrum $\hat{G}(\Delta\kappa)=(2\pi)^{-1/2}\int dxG(x)\exp(-i\kappa x)$ and near-field distribution $G(x)$. In this case we may write

$$g^{(l)}(x,0;\kappa_0) = \frac{1}{\sqrt{2\pi}}\int d\Delta\kappa\hat{G}(\Delta\kappa)$$

$$\times\exp\left(i\kappa_0 x+i\Delta\kappa x+i\frac{2\pi}{a}lx\right). \quad (A7)$$

Repeating the previous analysis to each of the plane waves entering in the integral on the right-hand side of Eq. (A7) and using the superposition principle yields

$$g^{(l)}(x,z_B;\kappa_0) = \sum_{\rho=0,\pm1,\pm2,\dots}\int d\Delta\kappa\frac{1}{\sqrt{2\pi}}\hat{G}(\Delta\kappa)\mathcal{M}_{l,\rho}$$

$$\times(\kappa_0+\Delta\kappa)\exp\left(i\kappa_0 x+i\Delta\kappa x+i\frac{2\pi}{a}\rho x\right).$$

$$(A8)$$

If the Fourier coefficients $\theta_{n,l}(\kappa)$ of Bloch states—and hence the transfer matrix $\mathcal{M}(\kappa)$—vary slowly over the spectral extension of $\hat{G}(\Delta\kappa)$, we may take $\mathcal{M}_{l,\rho}(\kappa_0+\Delta\kappa)\simeq\mathcal{M}_{l,\rho}(\kappa_0)$ out of the integral in Eq. (A8). The remaining terms left under the integral then yields precisely $g^{(\rho)}(x,0;\kappa_0)$ [see Eq. (A7)]. We thus finally obtain

$$g^{(l)}(x,z_B;\kappa_0) = \sum_{\rho=0,\pm1,\pm2,\dots}\mathcal{M}_{l,\rho}(\kappa_0)g^{(\rho)}(x,0;\kappa_0), \quad (A9)$$

which extends the scattering matrix formalism to the case of broad beam excitation.

*longhi@fisi.polimi.it

[1] F. Bloch, Z. Phys. **52**, 555 (1928); C. Zener, Proc. R. Soc. London, Ser. A **145**, 523 (1934); G. H. Wannier, Phys. Rev. **117**, 432 (1960).

[2] E. E. Mendez, F. Agullo-Rueda, and J. M. Hong, Phys. Rev. Lett. **60**, 2426 (1988); J. Feldmann, K. Leo, J. Shah, D. A. B. Miller, J. E. Cunningham, T. Meier, G. von Plessen, A. Schulze, P. Thomas, and S. Schmitt-Rink, Phys. Rev. B **46**, 7252 (1992); K. Leo, Semicond. Sci. Technol. **13**, 249 (1998); M. Glück, A. R. Kolovsky, and H. J. Korsch, Phys. Rep. **366**, 103 (2002).

[3] M. Ben Dahan, E. Peik, J. Reichel, Y. Castin, and C. Salomon, Phys. Rev. Lett. **76**, 4508 (1996); B. P. Anderson and M. A. Kasevich, Science **282**, 1686 (1998).

[4] R. Morandotti, U. Peschel, J. S. Aitchison, H. S. Eisenberg, and Y. Silberberg, Phys. Rev. Lett. **83**, 4756 (1999); T. Pertsch, P. Dannberg, W. Elflein, A. Bräuer, and F. Lederer, *ibid.* **83**, 4752 (1999).

[5] G. Monsivais, M. del Castillo-Mussot, and F. Claro, Phys. Rev. Lett. **64**, 1433 (1990); G. Malpuech, A. Kavokin, G. Panzarini, and A. Di Carlo, Phys. Rev. B **63**, 035108 (2001); R. Sapienza, P. Costantino, D. Wiersma, M. Ghulinyan, C. J. Oton, and L. Pavesi, Phys. Rev. Lett. **91**, 263902 (2003); V. Agarwal, J. A. del Rio, G. Malpuech, M. Zamfirescu, A. Kavokin, D. Coquillat, D. Scalbert, M. Vladimirova, and B. Gil, *ibid.* **92**, 097401 (2004); M. Ghulinyan, C. J. Oton, Z. Gaburro, L. Pavesi, C. Toninelli, and D. S. Wiersma, *ibid.* **94**, 127401 (2005); V. Lousse and S. Fan, Phys. Rev. B **72**, 075119 (2005).

[6] D. N. Christodoulides, F. Lederer, and Y. Silberberg, Nature (London) **424**, 817 (2003).

[7] H. Trompeter, T. Pertsch, F. Lederer, D. Michaelis, U. Streppel, A. Bräuer, and U. Peschel, Phys. Rev. Lett. **96**, 023901 (2006); N. Chiodo, G. DellaValle, R. Osellame, S. Longhi, G. Cerullo, R. Ramponi, P. Laporta, and U. Morgner, Opt. Lett. **31**, 1651 (2006).

[8] H. Sanchis-Alepuz, Y. A. Kosevich, and J. Sanchez-Dehesa, Phys. Rev. Lett. **98**, 134301 (2007); Z. He, S. Peng, F. Cai, M. Ke, and Z. Liu, Phys. Rev. E **76**, 056605 (2007).

[9] W. Lin, X. Zhou, G. P. Wang, and C. T. Chan, Appl. Phys. Lett. **91**, 243113 (2007); A. R. Davoyan, I. V. Shadrivov, A. A. Sukhorukov, and Y. S. Kivshar, Opt. Express **16**, 3299 (2008); A. R. Davoyan, A. A. Sukhorukov, I. V. Shadrivov, and Y. S. Kivshar, Phys. Rev. A **79**, 013820 (2009).

[10] B. M. Breid, D. Witthaut, and H. J. Korsch, New J. Phys. **8**, 110 (2006).

[11] F. Dreisow, A. Szameit, M. Heinrich, T. Pertsch, S. Nolte, A. Tünnermann, and S. Longhi, Phys. Rev. Lett. **102**, 076802 (2009).

[12] B. M. Breid, D. Witthaut, and H. J. Korsch, New J. Phys. **9**, 62 (2007).

[13] J. Janszky, C. Sibilia, and M. Bertolotti, J. Mod. Opt. **35**, 1757 (1988); W. K. Lai, V. Bužek, and P. L. Knight, Phys. Rev. A **43**, 6323 (1991); A. Bandyopadhyay and J. Rai, Opt. Commun. **140**, 41 (1997).

[14] A. Politi, M. J. Cryan, J. G. Rarity, S. Yu, and J. L. O'Brien, Science **320**, 646 (2008).

[15] S. Longhi, Phys. Rev. Lett. **101**, 193902 (2008).

[16] A. Rai and G. S. Agarwal, Phys. Rev. A **79**, 053849 (2009).

[17] C. K. Hong, Z. Y. Ou, and L. Mandel, Phys. Rev. Lett. **59**, 2044 (1987).

[18] Y. Bromberg, Y. Lahini, R. Morandotti, and Y. Silberberg, arXiv:0807.3938 (unpublished).

[19] A. Rai, G. S. Agarwal, and J. H. H. Perk, Phys. Rev. A **78**, 042304 (2008).

[20] J. G. Rarity, P. R. Tapster, E. Jakeman, T. Larchuk, R. A. Campos, M. C. Teich, and B. E. A. Saleh, Phys. Rev. Lett. **65**, 1348 (1990).

[21] A. N. Boto, P. Kok, D. S. Abrams, S. L. Braunstein, C. P. Williams, and J. P. Dowling, Phys. Rev. Lett. **85**, 2733 (2000).

[22] K. Edamatsu, R. Shimizu, and T. Itoh, Phys. Rev. Lett. **89**, 213601 (2002).

[23] P. Walther and J.-W. Pan, M. Aspelmeyer, R. Ursin, S. Gasparoni, and A. Zeilinger, Nature (London) **429**, 158 (2004).

[24] S. Longhi, M. Lobino, M. Marangoni, R. Ramponi, P. Laporta, E. Cianci, and V. Foglietti, Phys. Rev. B **74**, 155116 (2006); S. Longhi, Europhys. Lett. **76**, 416 (2006).

[25] J. Callaway, *Quantum Theory of the Solid State* (Academic, New York, 1974), pp. 465–478.

[26] J. Zak, Phys. Rev. Lett. **62**, 2747 (1989).

[27] For a symmetric refractive index profile of the waveguide, such as for the lattice of Fig. 1(b), the periodic part $u_n(x,\kappa)$ of Bloch states can be chosen such that $E_n'(\kappa)=E_n(\kappa)$ and the Berry phase correction to γ_n vanishes.

[28] The tilt and Bragg angles θ and θ_B are here measured for light waves propagating inside the dielectric medium of refractive index n_s rather than in vacuum, as in Ref. 24.

[29] R. A. Campos, B. E. A. Saleh, and M. C. Teich, Phys. Rev. A **40**, 1371 (1989).

[30] In polymer waveguide arrays, tuning of the index gradient F can be realized by thermal gradient control, as demonstrated in the experiments of Refs. 4 and 7. In lithium-niobate waveguide arrays, such as those used in the experiment of Ref. 24, electro-optic tuning of the phase difference $\Delta\gamma$ can be also achieved.

[31] Y. Lai and H. A. Haus, Phys. Rev. A **40**, 844 (1989); E. M. Wright, *ibid.* **43**, 3836 (1991); P. L. Hagelstein, *ibid.* **54**, 2426 (1996); A. B. Matsko and V. V. Kozlov, *ibid.* **62**, 033811 (2000).

[32] S. Longhi, Phys. Rev. A **79**, 023811 (2009).

[33] U. Leonhardt, Rep. Prog. Phys. **66**, 1207 (2003); J. Skaar, J. C. G. Escartin, and H. Landro, Am. J. Phys. **72**, 1385 (2004).

[34] The classical interference fringes, oscillationg like $\sim\cos(\Delta\gamma)$, are retrieved when the quantum state of the input field is in a coherent state, or when a single photon, in either one of the two beams g_1 or g_2, undergoes a two-band BO cycle, i.e., for either $|\mathcal{Q}(z=0)\rangle=|1\rangle_1|0\rangle_2$ or $|\mathcal{Q}(z=0)\rangle=|0\rangle_1|1\rangle_2$.